# Perturbation mechanism and phase transition of AOT aggregates in the Fe(II)[batho(SO$_3$)$_2$]$_3$ - catalyzed aqueous Belousov-Zhabotinsky reaction

Rumana A. Jahan [a,b], Kosuke Suzuki [a,b], Hitoshi Mahara [a], Satoshi Nishimura [a], Takashi Iwatsubo [a], Akiko Kaminaga [c], Yasuhiko Yamamoto [b], Tomohiko Yamaguchi [a,*]

[a] *National Institute of Advanced Industrial Science and Technology, 1-1-1 Higashi, Tsukuba 305-8565, Japan*
[b] *Department of Chemistry, Graduate School of Pure and Applied Science, University of Tsukuba, 1-1-1 Tennodai, Tsukuba 305-8571, Japan*
[c] *Department of Chemistry and Bioscience, Faculty of Science, Kagoshima University, 1-21-35 Korimoto, Kagoshima 890-0065, Japan*

\* Corresponding author. Fax +81-29-861-6236.

*E-mail addres*s: tomo.yamaguchi@aist.go.jp (T. Yamaguchi).

**ABSTRACT**

Surfactant AOT (sodium bis(2-ethylhexyl)sulfosuccinate) was introduced up to 200 mmol $L^{-1}$ in the aqueous Belousov-Zhabotinsky (BZ) medium. Both the induction period (IP) and the oscillation period ($\tau$) of the BZ waves decreased significantly, whereas the wave velocity ($v$) increased with the concentration of AOT. These tendencies were explained in terms of the perturbations to the FKN mechanism through the uptake of $Br_2$ and $BrO_2^{\bullet}$ into the hydrophobic core of AOT aggregates. In addition, the structures and the phase transition of AOT aggregates were suggested based on the measurement of surface tension and the correlation analysis of the IP, $\tau$ and $v$ values.

Rumana  et.al.

## 1. Introduction

The Belousov-Zhabotinsky (BZ) reaction is the most famous and thoroughly studied nonlinear reaction that produces temporal oscillations and a variety of spatio-temporal patterns in laboratory experiments [1,2]. These patterns include concentric and spiral travelling chemical waves and Turing patterns. The BZ reaction generally represents the catalytic oxidation of an organic substrate by bromate ($BrO_3^-$) in the presence of metal catalyst in a strongly acidic aqueous solution, and it is often regarded as a chemical model of biological pattern dynamics [3,4].

A perturbation given to the system often brings about macroscopic changes in the spatio-temporal behaviors of the BZ reaction [5]. Light [6-11] and oxygen [12] directly interact with the chemical species in the BZ reaction to inhibit the reaction. Even an addition of non-reacting chemical species induces effective changes in the pattern dynamics. For example, self-assembled aggregates of surfactants have been employed to compartmentalize crucial intermediates to affect the temporal dynamics of the BZ reaction [13-16]. These perturbation experiments often give us a new insight about the reaction mechanism in addition to the controllability of the pattern dynamics.

Here, we investigate the pattern dynamics of an aqueous BZ system perturbed by introducing a strong surfactant: AOT (sodium bis(2-ethylhexyl)sulfosuccinate). AOT is composed of an anionic headgroup ($-SO_3^-$) and two hydrocarbon tails (Fig. 1a), and has been used successfully for constructing the reverse-micelles BZ systems in octane

[17-19]. In an aqueous system, contrarily, it self-assembles into hydrophobic aggregates that may work as a pool to accumulate hydrophobic intermediates in the BZ reaction. It is also noteworthy that AOT in water forms different kinds of self-assembled structures depending on its concentration [20,21]. Such morphological changes are reasonably expected to affect the BZ patterns if the hydrophobicity of AOT-aggregates becomes varied with their shape and size.

In the present work, we vary the concentration of AOT up to 200 mmol $L^{-1}$ in an aqueous BZ system, and attempt to deduce the perturbation mechanism of AOT through the experimental results on the induction period (IP), the oscillation period ($\tau$), and the velocity normal to the wave front of the BZ patterns ($v$). In the present system, the induction period is defined as the time required for the waves to emerge after mixing all the chemicals. It is known that the dynamics of BZ patterns is well-described by the reaction-diffusion mechanism [22], where the diffusion obeys Fick's second law and the reaction does the so-called FKN mechanism [23]. We follow the original FKN mechanism but introduce a slight change in Process A so that the three processes proceed sequentially with time:

Process A*: reducing the concentration of $Br^-$ to produce $Br_2$ and the necessary amount of autocatalytic species $HBrO_2$ for kicking off the next process. In addition to the reactions in the original Process A of FKN mechanism, the present process A* includes the bromination reaction of malonic acid (MA) by $Br_2$. This reaction takes place instantaneously to produce bromomalonic acid (BrMA).

Rumana et.al.

Process B: autocatalytic production of $HBrO_2$ by reduction of $BrO_3^-$. Since this autocatalytic step is accompanied by the production of radical $BrO_2^\bullet$, oxidation of metal catalyst takes place by single electron transfer.

Process C: oxidation of MA and BrMA by the oxidized catalyst, which eventually turns back to its reduced state. This redox reaction is associated with reproduction of $Br^-$.

Process A* determines the IP; Process B is related to the $v$ that is also a function of diffusion coefficient of $HBrO_2$; Process C is the most responsible for the oscillation period $\tau$ [24].


## 2. Experimental


Malonic acid (MA), sodium bromate ($NaBrO_3$) and sulfuric acid were of reagent grade purchased from Wako Pure Chem. Ind. Ltd. Bathoferroin hexasulfonate ($Fe(II)[batho(SO_3)_2]_3$) (Fig.1b), called bathoferroin hereafter, were prepared by stoichiometric mixing of 4,7-diphenyl-1,10-phenanthroline disulfonic acid sodium salt (Nacalai Tesque Inc.) with ferrous sulfate・$7H_2O$ (Wako) in 3:1 molar ratio in water to yield the complex at the concentration of 25 mmol $L^{-1}$ of the catalyst. Sodium bis(2-ethylhexyl)sulfosuccinate (AOT; Sigma-Aldrich) was of the highest purity available and used without further purification. It was stored sealed by parafilm in a desiccator since the reagent is highly hygroscopic.

The BZ solutions ([MA]: 0.25 mol $L^{-1}$, [$H^+$]: 0.20 mol $L^{-1}$,

[NaBrO$_3$]: 0.18 mol L$^{-1}$, [bathoferroin]: 4 mmol L$^{-1}$) were prepared from the aqueous stock solutions of 2 mol L$^{-1}$ MA (malonic acid), 5 mol L$^{-1}$ H$_2$SO$_4$, 1 mol L$^{-1}$ NaBrO$_3$ and 25 mmol L$^{-1}$ of bathoferroin. An aqueous solution of the anionic surfactant AOT (400 mmol L$^{-1}$) was used as a stock solution. Milli-Q doubly distilled water was used to prepare all the aqueous solutions in the present work. A fixed volume (30 μL) of reaction medium was placed between two glass plates spaced by 0.8 mm. This uniform geometrical condition was achieved by using commercially available glass plates (UR-137-S) purchased from Sekisui Chemicals Co. Ltd. The experiments were performed at room temperature, 24 ± 1 °C.

The time evolution of BZ patterns was monitored under microscope (Leica WILD MZ8) equipped with a spatially-homogeneous cold backlight (metal halide lamp, PCS-UMX350, Nippon P.I Co., Ltd. with flat light guide PLG-B100X) and a CCD camera (SONY XC-77, driven by an image controller HAMAMATSU C-2400). The images were digitized on a PC and processed for further analysis. The values of $\tau$ and $v$ of the BZ waves were determined by constructing the space-time diagrams from the sequential images of traveling waves. Experiments were conducted five times for each condition.

The values of critical micelles concentration (CMC) of AOT in pure water and in the BZ solutions were determined by the surface tension ($\gamma$) measurements. This was conducted by applying the Wilhelmy plate method at 24 ± 1 °C using an electro surface balance (Model ESB-V, Kyowa Scientific Co. Ltd.) equipped with a platinum plate.

Rumana et.al.

## 3. Results

The replacement of the classical BZ catalyst $Fe(II)(phen)_3$ (i.e., ferroin) by $Fe(II)[batho(SO_3)_2]_3$ (bathoferroin) [25] proved to be an effective substitution for our experimental system. The major reason for using bathoferroin instead of ferroin in this work is that the positively-charged ferroin interacts with the anionic surfactant to result in the formation of adducts especially at high concentration of AOT (Fig. 2g). The BZ waves observed were in good contrast by use of bathoferroin. The wavelength of the BZ patterns became substantially shorter with increasing concentration of AOT (Fig. 2a – 2f).

Three characteristic measures of the BZ waves were determined in the presence of AOT up to 200 mmol $L^{-1}$: the induction period IP (Fig. 3a), the normal velocity of the propagating BZ waves $v$ (Fig. 3b), and the period of oscillations $\tau$ (Fig. 3c). The results obtained at low concentrations of AOT (0 – 25 mmol $L^{-1}$), given as insets, illustrate that IP decreased only slightly with the concentration of AOT; $v$ increased slightly, and $\tau$ decreased gradually. On the other hand, at high concentrations of AOT (~ 200 mmol $L^{-1}$), sharp decreases were observed in both values of IP and $\tau$, whereas the profile of $v$ did not show such clear tendency. The present tendency in $v$ is different from that reported in the case of another anionic surfactant: sodium dodecyl sulfate (SDS) [15].

The CMC value of AOT in the presence of BZ reactants was 0.68 mmol $L^{-1}$ (Fig. 4), whereas the value in pure water was obtained as 2.3 mmol $L^{-1}$. The latter is in good agreement with the known value of 2.5

Rumana et.al.

mmol $L^{-1}$ [21]. The lower value of CMC in the BZ solution is due to the high ionic strength [26,27]. Further measurement at AOT concentration much higher than 60 mmol $L^{-1}$ was practically difficult by the present Wilhelmy plate method.

## 4. Discussion

### 4.1.  Perturbation mechanism of AOT aggregates

The induction period IP is under the control of Process A* in the FKN mechanism. The major role of Process A* is to decrease the concentration of inhibitor $Br^-$ to produce $Br_2$, HOBr and $HBrO_2$ according to the reactions R1 (Eq. (1) below), R2, and R3 in the classical FKN mechanism [23], respectively. Since $Br_2$ is highly hydrophobic, it is absorbed into the hydrophobic core of AOT aggregates (Eq. (2)).

$$Br^- + HOBr + H^+ \Leftrightarrow Br_2 + H_2O \tag{1}$$
$$Br_2 + AOT(ag) \Leftrightarrow Br_2 \subset AOT(ag) \tag{2}$$

Here AOT(ag) stands for the aggregated phase of AOT. Equation (2) accelerates the decreasing rate of $Br^-$ concentration due to the mass action law in Eq. (1), and consequently decreases the induction time. According to this perturbation mechanism, the induction time decreases almost proportionally to the amount of AOT aggregates. This tendency has been confirmed by numerical calculations of Process A* (data not shown).

Rumana et.al.

Next, in order to corroborate the effect of the hydrophobic phase on the oscillation period $\tau$, we conduct numerical calculations of oscillatory medium by using the two-variable Rovinsky-Zhabotinsky (RZ) model [28] that is known as a good model for the ferroin-catalyzed BZ system. After Vanag et al. [19], we include the concentration of hydrophobic intermediate $BrO_2^{\bullet}$ as the third variable $s$ to take the autocatalytic process into account in the hydrophobic subphase:

$$\frac{dx}{dt} = \left\{ x(1-x) - (2q\alpha \frac{z}{1-z} \frac{x-\mu}{x+\mu}) \right\} / \varepsilon - k_f x + k_b s, \tag{3}$$

$$\frac{dz}{dt} = x - \alpha \frac{z}{1-z}, \tag{4}$$

$$\frac{ds}{dt} = k_f x - k_b s + \phi s, \tag{5}$$

where $x = [HBrO_2]$, $z = [Fe(III)[batho(SO_3)_2]_3^{3-}]$, and $s = [BrO_2^{\bullet}]$; $\varepsilon = k_1 A / k_4 C$, $\alpha = k_4 k_8 B / k_1^2 A^2 h_0^2$, and $\mu = 2k_4 k_7 / k_1 k_5$, where $A = [HBrO_3]$, $B = [BrMA]$, $C$ is the total concentration of catalyst; $k_i$ ($i = 1 - 8$) is the rate constant; $h_0$ is the acidity function and $q$ is the stoichiometric factor; $k_f$ and $k_b$ are the rate constants of the forward and the backward reaction of $BrO_2^{\bullet}$ production in an aqueous phase, respectively. The influence of AOT aggregate is represented by $\phi$, which is regarded as proportional to the volume ratio of AOT to water. In the present model, the rate constant of the autocatalytic process is written as $k_1$ (see Ref. [28]).

As shown in Fig. 3d, a decrease similar to the experimental results in

Rumana et.al.

Fig. 3c is observed in the profile of oscillation period $\tau$. This good agreement is qualitatively explained as follows. By application of the quasi-steady state assumption to Eqs. (3) and (5) in Process C, where $x$ is sufficiently smaller than $\mu$ ($<<$ 1), we obtain the reduction rate of oxidized catalyst as a function of $z$ and $s$:

$$-\left(\frac{\mathrm{d}z}{\mathrm{d}t}\right)_{\mathrm{C}} \approx \alpha\ (1+2q)\left(\frac{z}{1-z}\right)+\varepsilon\ \phi\ s. \tag{6}$$

The first term on the right-hand side arises from the original RZ model, and the second term from Eq. (5), where $\phi\,s$ represents the autocatalytic production of $BrO_2^\bullet$ in the presence of hydrophobic subphase. Equation (6) means that the rate $-(\mathrm{d}z/\mathrm{d}t)_{\mathrm{C}}$ increases linearly with the value of $\phi$, and consequently, the period of Process C decreases with $\phi$. Since the value of the oscillation period is mainly determined by the duration time of Process C [24], $\tau$ decreases with $\phi$. In this way, the decrease in the oscillation period is explained by the increase in the reduction rate of Process C, which is brought about by the distribution of hydrophobic $BrO_2^\bullet$ into AOT aggregates.

Finally, we deal with the change in the wave velocity $v$ that is tightly related to the autocatalytic Process B. There is a well-known relation about the velocity of the BZ wave:

$$v_{\mathrm{p}} \propto (kD)^{0.5}, \tag{7}$$

where $v_p$ is the velocity of the planar BZ wave, and $v = v_p$ when the curvature of the wave front is small enough; $k$ is the rate constant of the following autocatalytic reaction, and $D$ is the apparent diffusion coefficient of autocatalytic species [29,30]:

$$HBrO_2 + BrO_3^- + H^+ \Leftrightarrow 2BrO_2^{\bullet} + H_2O \qquad (8)$$

Here, $k$ is little influenced by AOT because of the small value of $\varepsilon$ in Eq. (3), whereas $D$ may change with $\phi$. As mentioned above, the autocatalytic species $BrO_2^{\bullet}$ is accumulated in the hydrophobic core of AOT aggregates to decrease the values of $\tau$. This accumulation simultaneously contributes to lessen the necessary amount of $HBrO_2$ that diffuses in front of the oxidative wave to sustain the wave propagation. Alternatively, the influence of $HBrO_2$ reaches to a longer distance by diffusion. In this way, even if the value of diffusion coefficient remains the same, the apparent value of $D$ may increase and result in the linear increase in $v$ with the amount of AOT.

### 4.2. *Phase transition of AOT aggregates*

Figure 4 shows the dependence of the values of the surface tension $\gamma$ and the induction period IP on the concentration of AOT. The wide plateau of the $\gamma$ values above the CMC (0.68 mmol L$^{-1}$) indicates that the concentration of free AOT is constant, and above CMC, the amount of AOT aggregates (spherical micelles) increases with the increase in AOT.

Therefore, one can reasonably say that the decrease in the IP value is caused by the increase in the concentration of AOT micelles, and the change in the slope around 6 mmol $L^{-1}$ suggests the phase transition associated with the structural change of AOT micelles. As X-ray diffraction analysis revealed no lamellar structures (data not shown), this is most probably due to the phase transition from spherical micelles to rod-like micelles [20]. At AOT concentrations much higher than 60 mmol $L^{-1}$, IP decreases very sharply (Fig. 3a). It suggests the appearance of new phases, which can be depicted by the following correlation analysis.

The correlation between the IP and $\tau$ values appears as a monotonically increasing line with two kinks (Fig. 5a). This diagram illustrates the strong positive correlation between the lengths of Process A* and Process C in the FKN mechanism. The tri-phase line in Fig. 5a suggests the existence of at least three phases in AOT aggregates that correspond to the concentrations of $0 - 60$ mmol $L^{-1}$, $60 - 100$ mmol $L^{-1}$ and above 100 mmol $L^{-1}$. The former two are also noticeable in Fig. 3a, but the third one becomes clear from this correlation plots. The linear correlation in $0 - 60$ mmol $L^{-1}$ implies only little change in the hydrophobicity of AOT aggregates, which supports the phase transition from spherical to rod-like micelles at 6.0 mmol $L^{-1}$. Above 100 mmol $L^{-1}$, the BZ medium scattered a laser beam due to the emergence of macroscopic AOT aggregates which was visible under optical microscope. If the size of these macroscopic aggregates becomes large enough, they may trigger the BZ waves [31,32] to lessen both the values of IP and $\tau$.

The plots of $v$ against IP appear as a broken line with a negative

Rumana et.al.

slope (Fig. 5b), suggesting the negative correlation between Process B and Process A*. The disorder in the middle region corresponds to the AOT concentration of 60 – 100 mmol $L^{-1}$. As there is no disorder in the correlation plots between Process A* and Process C (Fig. 5a), this disorder is induced something influential only to the wave velocity. The most probable reason is the increase in apparent diffusion due to the fluctuation (or disorder) of AOT aggregates, though little evidence is presently at hand.

In summary, AOT in the present BZ medium seems to exist in five states; free molecules at 0 – 0.68 mmol $L^{-1}$, spherical micelles at 0.68 – 6 mmol $L^{-1}$, rod-like micelles at 6 – 60 mmol $L^{-1}$, a transient disordered state at 60 – 100 mmol $L^{-1}$, and coexistence of macroscopic aggregates above 100 mmol $L^{-1}$.

## 5. Concluding remarks

Perturbation has been achieved to the aqueous BZ reaction system by introducing the anionic surfactant AOT. The values of induction period IP, oscillation period $\tau$ and wave velocity $v$ of the BZ patterns are changed significantly, and the extent of the change depends on the amount of AOT. We consider that the overall dynamics of the BZ reaction represented by the FKN mechanism is perturbed mainly through the hydrophobicity of AOT aggregates. The aggregates allow the distribution of $Br_2$ and $BrO_2^{\bullet}$ into their hydrophobic cores and decrease both IP and $\tau$ values, and increase the $v$ value.

As a future study remains the concrete study on the structural

transition of AOT aggregates associated with the change in their hydrophobicity, which has been suggested phenomenologically by the correlation analysis (Fig. 5). Electrostatic interaction between the charged BZ species and the surfactant aggregates may be another remaining issue to be addressed, though we consider it less influential than the hydrophobic interaction.

## Acknowledgments

## References

[1] A.N. Zaikin, A.M. Zhabotinsky, Nature 225 (1970) 535.

[2] R. Kapral, K. Showalter, Chemical Waves and Patterns, Kluwer Academic, Dordrecht, 1995.

[3] S. Kondo, R. Asai, Nature 376 (1995) 765.

[4] J.D. Lechleiter, L.M. John, P. Camacho, Biophys. Chem. 72 (1998) 123.

[5] M. Yoneyama, Chem. Phys. Lett. 254 (1996) 191.

[6] F. Bolletta, V. Balzani, J. Am. Chem. Soc. 104 (1984) 4250.

[7] I. Hanazaki, Y. Mori, T. Sekiguchi, G. Rabai, Physica D 84 (1995) 228.

[8] I. Hanazaki, J. Phys. Chem. 96 (13) (1992) 5652.

[9] V. Gaspar, G. Bazsa, M. Beck, Z. Phys. Chem. (Leipzig) 264 (1983) 43.

[10] T. Amemiya, S. Kadar, P. Kettunen, K. Showalter, Phys. Rev. Lett. 77 (1996) 3244.

[11] R. Toth, V. Gaspar, A. Belmonte, M.C. O'Connell, A. Taylor, S.K. Scott, Phys. Chem. Chem. Phys. 2 (2000) 413.

[12] A.F. Taylor, B.R. Johnson, S.K. Scott, Phys. Chem. Chem. Phys. 1 (1999) 807.

[13] A. Paul, J. Phys. Chem. B 109 (2005) 9639.

[14] L. Sciascia, R. Lombardo, M.L.T. Liveri, J. Phys. Chem. B 111 (2007) 1354.

[15] F. Rossi, R. Lombardo, L. Sciascia, C. Sbriziolo, M.L.T. Liveri, J. Phys. Chem. B 112 (2008) 7244.

[16] F. Rossi, R. Varsalona, M.L.T. Liveri, Chem. Phys. Lett. 463 (2008) 378.

[17] I.R. Epstein, V.K. Vanag, CHAOS 15 (2005) 047510.

[18] A. Kaminaga, V.K. Vanag, I.R. Epstein, J. Chem. Phys. 122 (2005)174706.

[19] V.K. Vanag, I.R. Epstein, Phys. Rev. Lett. 87 (2001) 228301.

[20] E.Y. Sheu, S-H. Chen, J.S. Huang, J. Phys. Chem. 91 (1987) 3306.

[21] E.F. Williams, N.T. Woodberry, J.K. Dixon, J. Colloid. Sci. 12 (1957) 452.

[22] J.D. Murray, Mathematical Biology, Springer-Verlag, Berlin, 2002.

[23] R.J. Field, E. Koros, R.M. Noyes, J. Am. Chem. Soc. 94 (25) (1972) 8649.

[24] J.J. Tyson, in: R.J. Field, M. Burger (Eds), Oscillations and Travelling

Waves in Chemical Systems, Wiley-Interscience, New York, 1985, p. 93.

[25] T. Yamaguchi, L. Kuhnert, Zs. Nagy-Ungvarai, S.C. Müller, B. Hess, J. Phys. Chem. 95 (1991) 5831.

[26] S.S. Rawat, S. Mukherjee, A. Chattopadhyay, J. Phys. Chem. B 101 (1997) 1922.

[27] I.M. Umlong, K. Ismail, J. Colloid Interface Sci. 291 (2005) 529.

[28] A.B. Rovinsky, A.M. Zhabotinsky, J. Phys. Chem. 88 (1984) 6081.

[29] R.J. Field, R.M. Noyes, J. Am. Chem. Soc. 96 (1974) 2001.

[30] R. Luther, R. Arnold, K. Showalter, J. Tyson, J. Chem. Educ. 64 (1987) 740.

[31] E. Mori, J. Ross, J. Phys. Chem. 96 (1992) 8053.

[32] P. Foerster, S. Müller, B. Hess, Proc. Natl. Acad. Sci. USA 86 (1989) 6831.

**Figure captions:**

**Fig. 1.** Chemical structure of (a) AOT (sodium bis(2-ethylhexyl)sulfosuccinate); (b) Fe(II)[bathophen(SO$_3$)$_2$]$_3$, abbreviated as bathoferroin in this work.
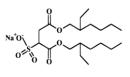
**Fig. 2.** Patterns without (a) and with 25 mmol L$^{-1}$ (b), 75 mmol L$^{-1}$ (c), 125 mmol L$^{-1}$ (d), 150 mmol L$^{-1}$ (e), and 175 mmol L$^{-1}$ (f) of AOT in the aqueous BZ system where [MA] = 0.25 mol L$^{-1}$, [H$_2$SO$_4$] = 0.2 mol L$^{-1}$, [NaBrO$_3$] = 0.18 mol L$^{-1}$, and [bathoferroin] = 4.0 mmol L$^{-1}$; (g) Hairy adducts formed at the interface of waxy AOT in contact with the BZ reactants containing ferroin. The white bars correspond to 1 mm. Temperature: 24 ± 1 °C.

**Fig. 3.** Influence of AOT concentration on: (a) the induction period IP, (b) the wave velocity $v$, and (c) the oscillation period $\tau$ of the BZ reaction. Each inset in (a) − (c) shows the expansion of each trend at low concentrations below 25 mmol L$^{-1}$. The lines are just for readers' guide. The profile (d) represents the simulated oscillation period ($\tau$) of the BZ reaction as a function of $\phi$ (a parameter proportional to the volume ratio of the hydrophobic subphase and aqueous phase), where the axes are given in arbitrary units.
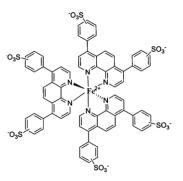
**Fig. 4.** Influence of AOT concentration on surface tension $\gamma$ (closed circle) and the induction period IP (open circle). Arrows A and B at 0.68 mmol L$^{-1}$ and 6.0 mmol L$^{-1}$ indicate the phase transition points in the surface tension (CMC) and the induction period, respectively. The inset expands the results of surface tension measurement at low concentrations of AOT.
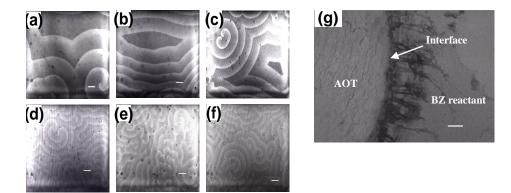
**Fig. 5.** Correlations: (a) between $\tau$ and IP; (b) between $v$ and IP of the BZ-AOT aqueous system. The lines drawn along the points are just for readers' guide to trail the existence of phase transitions in the system.
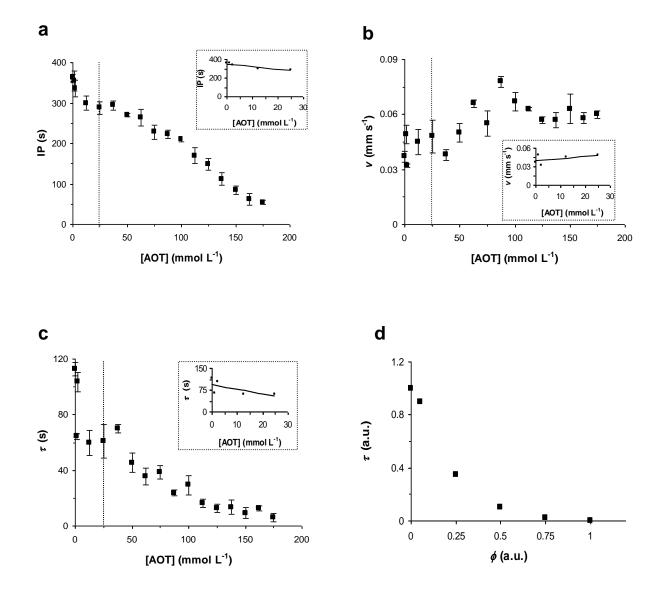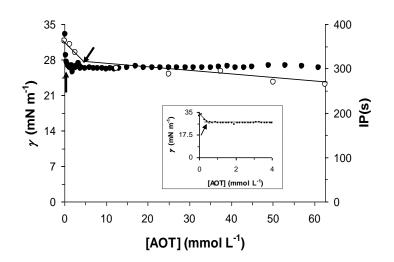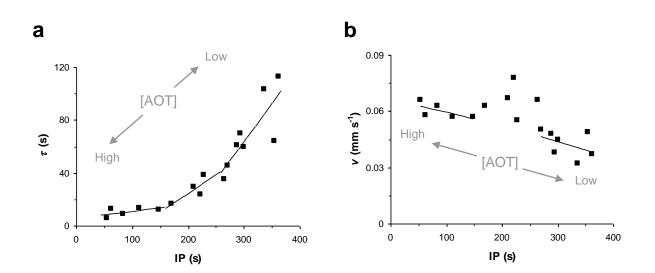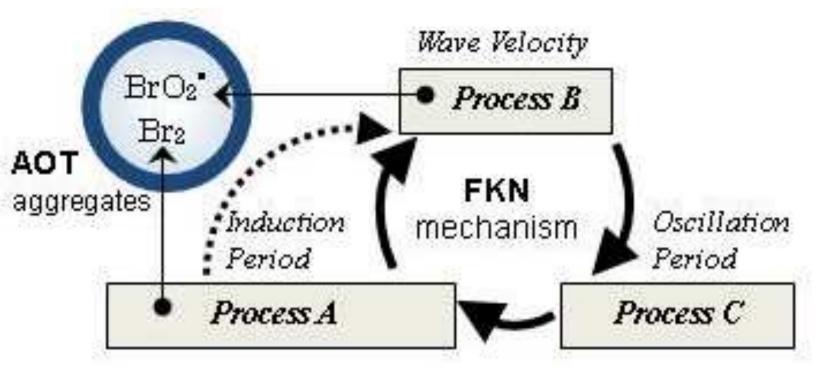
Rumana et.al.

**Figure 1**

**a**

**b**

**Figure 1**

Rumana et.al.

**Figure 2**



(a) (b) (c) (d) (e) (f) (g) Interface AOT BZ reactant

**Figure 2**

Rumana et.al.

**Figure 3**



**Figure 3**

1

Rumana et.al.

**Figure 4**



Figure 4

Rumana  et.al.

**Figure 5**

**a**



**b**



**Figure 5**

Rumana et.al.

Graphical Abstract (Synopsis):

The decrease in the induction period and the oscillation period, and the increase in the wave velocity observed are discussed in terms of FKN mechanism and the hydrophobicity of AOT (sodium bis(2-ethylhexyl)sulfosuccinate) accompanied by phase transitions.